Journal of General Virology (2012), **93**, 275–281 DOI 10.1099/vir.0.033589-0

Bat severe acute respiratory syndrome-like coronavirus ORF3b homologues display different interferon antagonist activities

Peng Zhou,[1] Hongxia Li,[1] Hanzhong Wang,[1] Lin-Fa Wang[2] and Zhengli Shi[1]

Correspondence
Zhengli Shi
zlshi@wh.iov.cn

[1]State Key Laboratory of Virology, Wuhan Institute of Virology, Chinese Academy of Sciences, Wuhan, Republic of China

[2]Australian Animal Health Laboratory, Commonwealth Scientific and Industrial Research Organisation Livestock Industries, Geelong, Victoria, Australia

The ORF3b protein of severe acute respiratory syndrome coronavirus (SARS-CoV) has a nuclear localization signal (NLS) at its C terminus and antagonizes interferon (IFN) function by modulating the activity of IFN regulatory factor 3 (IRF3). SARS-like coronaviruses (SL-CoVs) found in bats share an identical genome organization and high sequence identity for most of their gene products. In this study, ORF3b homologues were identified from three bat SL-CoV strains. These ORF3b homologues were C-terminally truncated and lacked the C-terminal NLS of SARS-CoV. IFN antagonist activities analysis demonstrated that one SL-CoV ORF3b still possessed IFN antagonist and IRF3-modulating activities. These results indicate that different ORF3b proteins display different IFN antagonist activities and this function is independent of the protein's nuclear localization, suggesting a potential link between bat SL-CoV ORF3b function and viral pathogenesis.

Received 26 April 2011
Accepted 18 October 2011

INTRODUCTION

The interferon (IFN) system functions as the first line of defence against viral infection in mammalian cells. Viral infection triggers a variety of cellular sensors that, in turn, activate a series of molecules, ultimately leading to the production of type I IFN (IFN-α and -β) (García-Sastre & Biron, 2006). One of these molecules, IFN regulatory factor 3 (IRF3), is essential for activation of the IFN-β gene promoter (Hiscott *et al.*, 1999; Randall & Goodbourn, 2008). IRF3 is expressed constitutively and localizes to the cytoplasm of uninfected cells. Upon activation by phosphorylation of its C-terminal domain mediated by TANK-binding kinase 1 (TBK1) and IκB kinase epsilon (IKKε) (Fitzgerald *et al.*, 2003), IRF3 translocates to the nucleus and promotes transcriptional activation. This activation leads to the production of IFN and several downstream antiviral genes, helping to establish an antiviral state.

To counteract the antiviral effects of IFN, viruses encode proteins to inhibit specific steps in IFN signalling or production (Basler *et al.*, 2003; Kochs *et al.*, 2007; Shaw *et al.*, 2004). Severe acute respiratory syndrome coronavirus (SARS-CoV), which emerged in 2003 and caused widespread mortality in humans, encodes at least five proteins that function as IFN antagonists (Devaraj *et al.*, 2007; Kamitani *et al.*, 2006; Kopecky-Bromberg *et al.*, 2007), suppressing components of both signalling and production. These proteins are believed to be responsible for the pathogenesis of SARS-CoV. Several strains of SARS-like coronavirus (SL-CoV) have been identified in horseshoe bats and found to be closely related to the human SARS-CoVs. SL-CoVs are believed to be members of a highly diverse coronavirus population in bats that includes the immediate ancestor of SARS-CoV (Lau *et al.*, 2005; Li *et al.*, 2005; Ren *et al.*, 2006). Bat SL-CoVs and human SARS-CoV share an identical genome organization and high sequence identity for most of their gene products. However, a synthesized recombinant SL-CoV caused no clinical disease in mice compared with SARS-CoV (Becker *et al.*, 2008), indicating a difference in pathogenesis between the two viruses, at least in mice.

SARS-CoV mRNA 3 encodes ORF3a and ORF3b proteins, both of which can be detected in SARS-CoV-infected tissues (Chan *et al.*, 2005). ORF3b shares a large part of its coding sequence with ORF3a with the exception of the C-terminal end (aa 134–154), which contains a nuclear localization signal (NLS). Despite the sequence similarity, ORF3a and ORF3b are translated in different reading frames and encode distinct proteins. SARS-CoV ORF3b, which encodes a 154 aa protein, has been shown to be an IFN antagonist (Kopecky-Bromberg *et al.*, 2007). ORF3b homologues have been identified for bat SL-CoV strains Rf1, Rm1 and Rp3 (Li *et al.*, 2005), but the three genes have different C-terminal truncations (Fig. 1). In this study, we

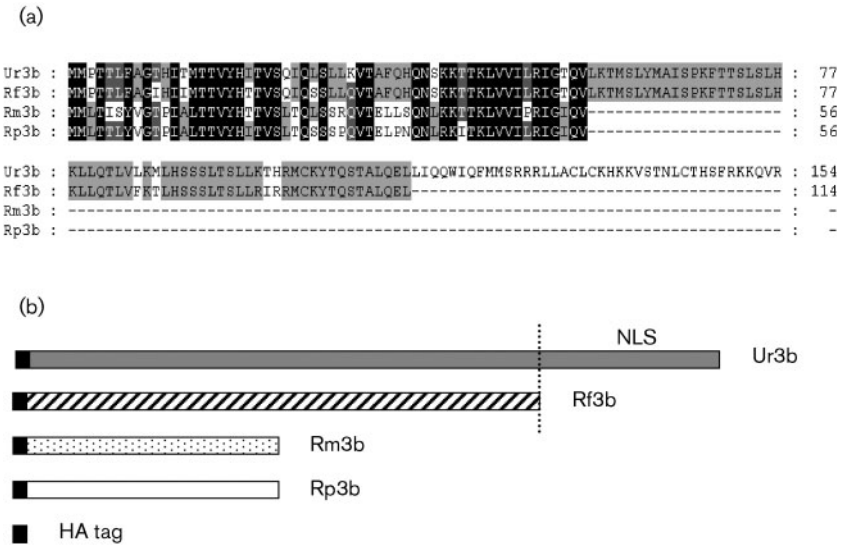

Fig. 1. Schematic diagram of human SARS-CoV and bat SL-CoV ORF3b proteins and expression constructs. (a) Alignment of SARS-CoV (Ur3b) and SL-CoV (Rf3b, Rm3b and Rp3b) ORF3b protein sequences. (b) Schematic diagram of ORF3b expression constructs used in this study. All ORF3b genes were fused in frame with the N-terminal haemagglutinin (HA) tag in pCAGGS. The region of Ur3b containing the NLS is indicated.

analysed the cellular localization and IFN antagonism of these ORF3b proteins and compared the results with those for SARS-CoV ORF3b.

RESULTS

Bat SL-CoV ORF3b homologues display different C-terminal truncations and different cellular locations

The ORF3b proteins from bat SL-CoV strains Rf1 (Rf3b), Rm1 (Rm3b) and Rp3 (Rp3b) were 114, 56 and 56 aa and shared amino acid sequence identities of 91, 62 and 64 %, respectively, with the ORF3b of SARS-CoV Urbani (Ur3b). The size differences were the result of a TAA stop codon in the SL-CoV ORF3b genes, leading to premature translation termination (Fig. 1).

For functional analyses, the ORF3b genes were cloned into a pCAGGS vector, which contains an N-terminal HA tag (Kochs *et al.*, 2007). Successful expression and cellular localization were analysed by Western blotting and confocal microscopy using an anti-HA antibody (Beyotime) (Fig. 2). For all the ORF3b constructs, the expressed proteins displayed a doublet in the Western blot (Fig. 2a), which was predicted to be the result of post-translational modification, although we are not sure which form of modification was responsible. However, we did detect a number of phosphorylation sites in the ORF3b sequences. To avoid cell toxicity caused by the over-expression of some gene constructs, a relatively short period of expression (16 h) was adopted, followed by immediate analysis after cell permeabilization. Unlike Ur3b, which was observed in the nucleus (Fig. 2b), all three SL-CoV ORF3b proteins (Rf3b, Rm3b and Rp3b) were found only in the cytoplasm (Fig. 2b). A putative NLS has been identified between aa 134 and 154 of Ur3b (Kopecky-Bromberg *et al.*, 2007; Yuan *et al.*, 2005). Thus, the cytoplasmic localization of the SL-CoV ORF3b proteins (Fig. 2) could be explained by their lack of an NLS.

Bat SL-CoV ORF3b homologues display different IFN antagonist activities

To investigate whether the SL-CoV ORF3b proteins are IFN antagonists despite their non-nuclear localization, we measured IFN-β promoter activation in response to Sendai virus (SeV) infection in the presence or absence of the ORF3b proteins. Human 293T cells were co-transfected with p125Luc (containing the IFN-β promoter fused to the firefly luciferase gene in a pGL3 vector), internal control plasmid pRL-TK (constitutively expressing *Renilla* luciferase) and a plasmid containing one of the following: ORF3b, influenza virus strain PR8 NS1 (positive control) (Kochs *et al.*, 2007) or no insert (empty negative-control vector). At 24 h post-transfection (p.t.), the cells were infected with SeV. At 18 h post-infection (p.i.), samples were analysed with a Dual-Luciferase Reporter Assay System (Promega). An aliquot of lysate was also examined for expression of ORF3b, and a pattern similar to those in Fig. 2(a) was observed (data not shown). Expression of the Rf3b gene resulted in severe cytotoxicity, preventing further analysis in this study.

Measurements of IFN-β activation inhibition are shown in Fig. 3(a). As expected, the positive control (NS1) demonstrated the strongest inhibition (almost 100 %), whilst Ur3b exhibited ~60 % inhibition. Interestingly, whilst Rp3b showed no inhibition at all, Rm3b demonstrated an inhibition equal to or better than that of Ur3b. The reduced luciferase activity was not a result of decreased cell viability among samples, shown by a comparison of cell morphology and production of *Renilla* luciferase, which served as an internal control. This observation was confirmed at the mRNA level by RT-PCR analysis (Fig. 3b).

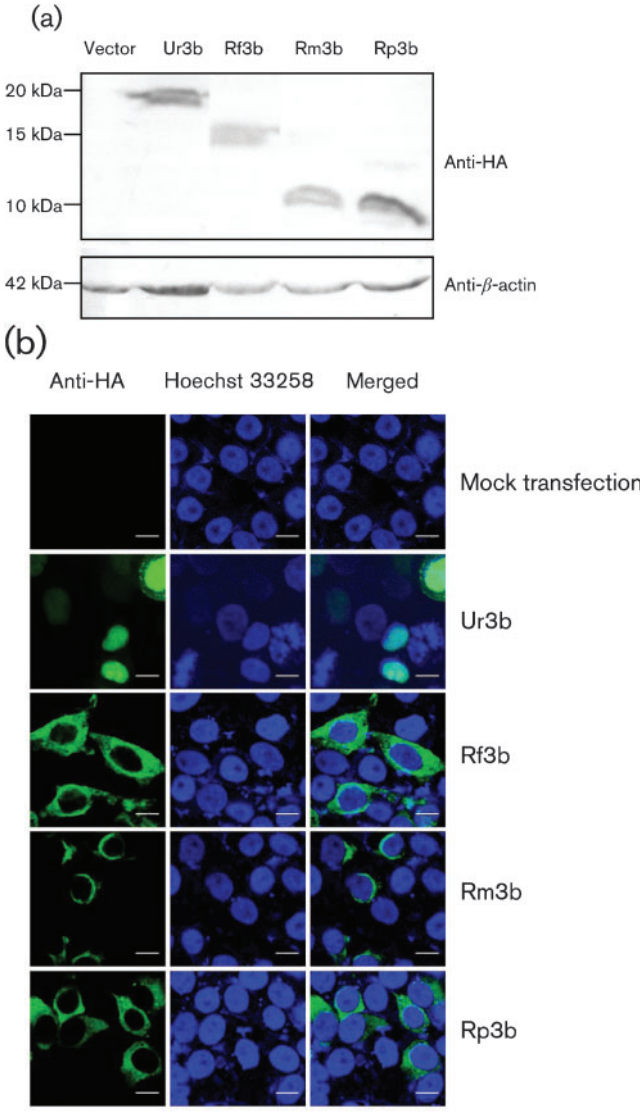

Fig. 2. Expression and subcellular localization of ORF3b proteins. (a) Western blot analysis of ORF3b proteins using an anti-HA mAb. Samples were normalized by measuring the relative amount of β-actin in the same sample. Sizes of the pre-stained molecular mass markers used in this study are indicated on the left. (b) Confocal microscopic analysis of HeLa cells in 24-well plates that had been incubated for 16 h after transfection with the plasmids indicated on the right. Hoechst 33258 was used to stain the nucleus. Merged images are shown on the right. Bars, 10 μm.

Rm3b inhibits activation of IRF3 differently from Ur3b

IRF3 is activated by phosphorylation of its C-terminal domain by TBK-1 and IKKε (Fitzgerald *et al.*, 2003), which allows it to be transported into the nucleus. As overexpression of either TBK-1 or IKKε had no effect on the inhibition profile of Ur3b or Rm3b (data not shown), we shifted our focus to IRF3. Cells were co-transfected with plasmids expressing IRF3, p125Luc, pRL-TK and either ORF3b or a control vector. At 24 h p.t., the cells were infected with SeV. After 18 h incubation, dual-luciferase activity was determined. An inhibition pattern was observed for constructs Rm3b, Ur3b and NS1, with NS1 showing the greatest inhibition, followed by Rm3b and Ur3b (Fig. 4a). We then examined the inhibition profile in the presence of IRF3(5D), a constitutively active mutant of IRF3 (Chang *et al.*, 2006). A similar inhibition profile was observed to that described above (Fig. 4b). In all cases, expression of the expected IRF3 and IRF3(5D) proteins was confirmed by Western blotting (data not shown). Taken together, these data suggested that, like Ur3b, Rm3b could inhibit IRF3-dependent IFN gene expression.

Ur3b is known to block the translocation of activated IRF3 from the cytoplasm to the nucleus (Kopecky-Bromberg *et al.*, 2007). To investigate whether Rm3b had the same function, the subcellular distribution of IRF3 was determined in the presence and absence of ORF3b proteins. HeLa cells were transfected with plasmids expressing NS1, Ur3b or Rm3b and incubated for 24 h, followed by SeV infection. After 8 h incubation, IRF3 distribution was determined by confocal immunofluorescence microscopy using a primary rabbit anti-IRF3 polyclonal antibody (Proteintech Group) and an FITC-conjugated goat anti-rabbit secondary antibody (Pierce). As shown in Fig. 4(c), IRF3 was localized to the cytoplasm of mock-infected cells. Upon SeV infection, the majority of IRF3 was translocated to the nucleus (90 %). This translocation was blocked to various degrees when NS1, Ur3b or Rm3b was co-expressed. An inhibition effect of 95, 88 and 96 % was determined, respectively, by counting labelled IRF3. To demonstrate further the effect of ORF3b in blocking IRF3 translocation, co-labelling of ORF3b and IRF3 was conducted. As shown in Fig. 4(d), whilst almost all Rm3b-expressing cells had IRF3 in the cytoplasm, some Ur3b-expressing cells had IRF3 in the nucleus, further indicating that Rm3b is more effective than Ur3b in blocking IRF3 translocation upon activation by viral (SeV) infection.

DISCUSSION

In this study, we showed that the ORF3b proteins of SARS-CoV and SL-CoV share substantial sequence identity and are co-linear at the N terminus, which is unique to ORF3b but not to ORF3a. Alignment of ORF3b proteins from different SARS-CoVs with bat SL-CoVs demonstrated that ORF3b was conserved at the N-terminal end among different SARS-CoVs, suggesting that they do encode virus proteins. However, the SL-CoV ORF3b proteins were smaller in size than SARS-CoV ORF3b due to truncations at the C termini from in-frame stop codons, and all three were cytoplasmic due to the lack of an NLS at the C terminus. Whilst mutations in Rp3, Rm1 and Rf1 caused early translation termination, they had minimal impact on the protein sequences of ORF3a (no change in the case of

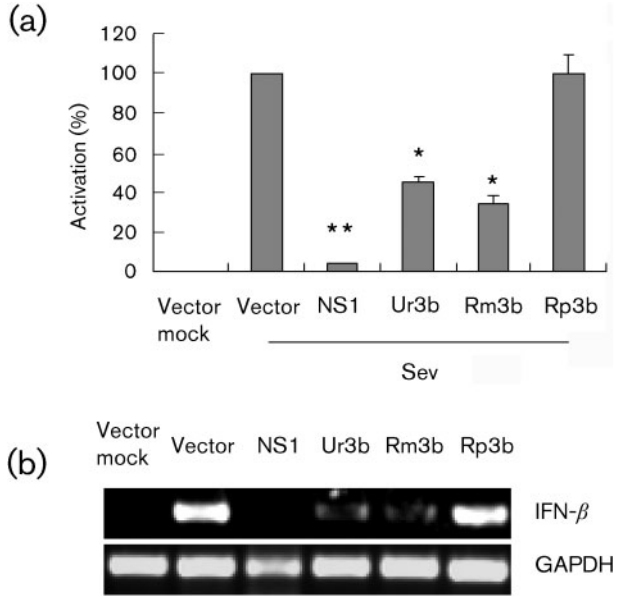

Fig. 3. Detection of IFN antagonist activity of ORF3b proteins. (a) Luciferase activity, which was used as a read-out of IFN-β promoter activation, was measured for cells containing the expression plasmids indicated on the figure. The analysis was conducted at 18 h p.i. SeV was added at 24 h p.t. The luciferase activity of the vector control was defined as 100 % activation. Data represent the means ± SEM of three experiments. *, $P<0.05$; **, $P<0.01$ versus vector (Student's *t*-test). (b) 293T cells in six-well dishes were transfected with 2.5 μg each of the indicated ORF3b plasmids for 24 h and then infected with 10 SeV HA units per well for 8 h. Total cellular RNA was extracted and the expression of IFN-β was measured by RT-PCR. Glyceraldehyde 3-phosphate dehydrogenase (GAPDH) was used as a control to ensure that RNA of comparable quality was analysed.

Rf1, 1 aa change in Rp3 and Rm1). Although the NLS-containing C-terminal end (aa 134–154) is the only ORF3b-specific region, it may not be important to its function as an IFN-β antagonist, as described previously (Freundt *et al.*, 2009) and observed in the present study. Furthermore, this C-terminal truncation in ORF3 also exists in other CoVs, such as infectious bronchitis virus, indicating that the CoV ORF3 is functionally tricistronic (Liu & Inglis, 1992; Liu *et al.*, 1991).

Interestingly, the three SL-CoV ORF3b proteins displayed very different activities with regard to IFN suppression. The largest SL-CoV ORF3b protein, Rf3b, was toxic to cells after incubation for 18 h or longer but did not induce cell apoptosis (data not shown). Of the two smaller SL-CoV ORF3b proteins, Rp3b showed no IFN antagonism, whereas Rm3b was a potent IFN antagonist that was even more active than Ur3b, the SARS-CoV ORF3b. Furthermore, we provided data to show that both Ur3b and Rm3b employ the same mechanism of IFN-β inhibition, blocking IRF3 translocation into the nucleus and thus preventing activation of the IFN-β gene promoter.

As a highly pathogenic virus, SARS-CoV encodes at least five proteins acting as IFN antagonists, including ORF3b, ORF6, nucleocapsid protein (Kopecky-Bromberg *et al.*, 2007) and a number of products of ORF1 (Devaraj *et al.*, 2007; Frieman *et al.*, 2009; Kamitani *et al.*, 2006). These proteins suppress IFN production or signalling through different mechanisms. With the exception of ORF3b, the bat SL-CoV homologues of these genes share high sequence identities with their SARS-CoV counterparts (Li *et al.*, 2005; Ren *et al.*, 2006). As attempts to isolate live SL-CoV have been uniformly unsuccessful to date, it is not possible to determine whether the different IFN-β antagonist activities of SL-CoV ORF3b observed in this study can be correlated with the pathogenicities of these viruses. In this regard, it is interesting to note that a recombinant SL-CoV virus (Bat-SRBD-MA) containing a truncated 39 aa ORF3b protein was non-pathogenic in aged mice (Becker *et al.*, 2008). Based on the results of our present study, we predict that this truncated ORF3b is unlikely to function as an IFN antagonist. It will be interesting to determine whether insertion of a functional ORF3b into Bat-SRBD-MA will have any effect on the pathogenicity of this recombinant virus.

Additionally, the NSP1 protein of SL-CoV Rm1 was shown recently to be a functional IFN antagonist (Tohya *et al.*, 2009). Taken together with our data, it can be concluded that both SL-CoV Rm1 and SARS-CoV share at least two homologous proteins that can function as IFN antagonists.

Considering the much smaller size of Rm3b compared with Ur3b and their different subcellular locations, we were surprised to find that Rm3b was more active than Ur3b as an IFN-β antagonist. Our study demonstrated that a C-terminal NLS is not required for an ORF3b protein to function as an IFN-β antagonist. This conclusion is supported by a recent report showing that the nuclear localization of Ur3b is not static; rather, the protein is shuttled between the nucleus and cytoplasm (Freundt *et al.*, 2009), which was also evident in our current study. At 32 h p.t., we observed substantial Ur3b in the cytoplasm (Fig. 4d). However, at 16 h p.t., the majority of Ur3b was nuclear (Fig. 2b). It seems reasonable to suggest that the main site of action for IFN antagonism by ORF3b is in the cytoplasm. Consequently, the biological significance of the NLS in Ur3b remains elusive at the present time. Our attempt to delete the NLS region in Ur3b, thus creating a molecule with the same size as Rf3b (114 aa), was unsuccessful because it was toxic to the cell system used in this study (as was Rf3b).

Finally, it should be noted that the IFN detection system used in this study was derived from and performed in human cells. Thus, it will be interesting to conduct the same studies in bat cells to determine whether these ORF3b homologues will have the same IFN antagonism profiles as those observed in the human cell system. The development of different *Rhinolophus* bat cell lines (Z. S., unpublished results; Crameri *et al.*, 2009), which is the reservoir host of SL-CoV, will facilitate this research in future.

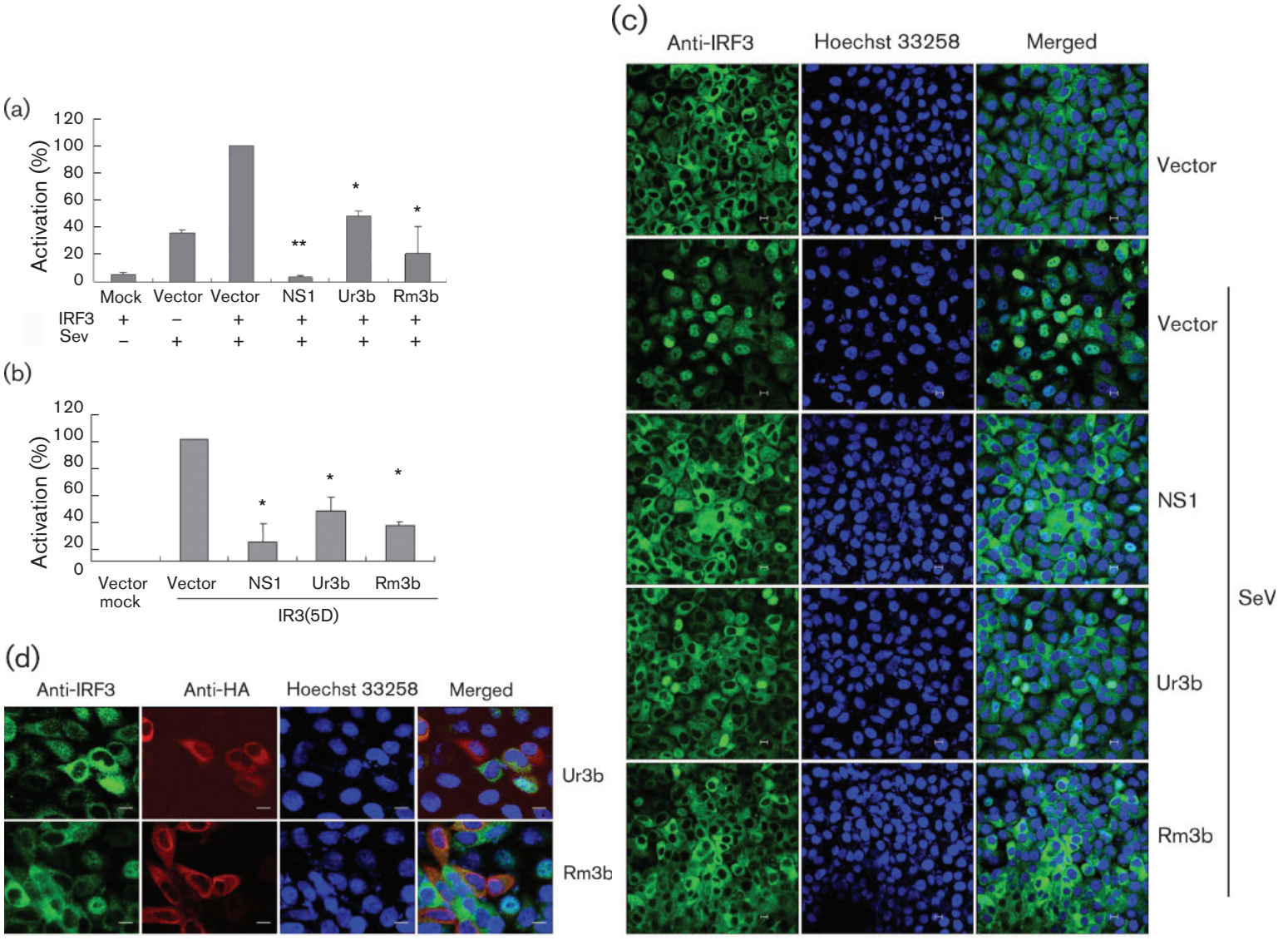

Fig. 4. Effect of Ur3b and Rm3b on IRF3 function. (a, b) Determination of IFN-β promoter activation in the presence of IRF3 and SeV (a) or IRF3(5D) (b). The analysis was conducted at 18 h p.i. SeV was added at 24 h p.t. Data are the means ± SEM of three experiments. *, $P<0.05$; **, $P<0.01$ versus vector (Student's *t*-test). (c, d) Confocal microscopic analysis of HeLa cells incubated for 24 h p.t. with different plasmids (indicated on the right) before infection with SeV. Analysis was conducted at 8 h p.i. Cells are stained as indicated above the images, using an antibody against IRF3 (c) or by dual labelling with antibodies against IRF3 and HA (d). Bars, 10 μm.

METHODS

Cells and virus. 293T and HeLa cells were cultured in Dulbecco's modified Eagle's medium (Gibco) containing 10 % FBS. SeV strain Cantell was grown in 10-day-old embryonated chicken eggs at 37 °C for 48 h.

Plasmids. Bat SL-CoV ORF3b genes (Rf1, Rm1 and Rp3) were amplified by PCR from SL-CoV plasmids constructed previously (Li *et al*., 2005). ORF3b of SARS-CoV was obtained from a SARS-CoV infectious cDNA clone. All the ORF3b genes were cloned into the pCAGGS vector constructed with an N-terminal HA tag. A positive control, plasmid pCAGGS-HA-NS1(PR8) encoding the NS1 protein of influenza strain PR8, was kindly provided by Dr Georg Kochs (Department of Virology, University of Freiburg, Germany). Successful expression of the proteins was confirmed by Western blotting using a mAb against the HA tag (Beyotime).

The plasmid p125Luc was constructed by inserting the IFN-β promoter (positions -125 to $+19$) fused to the firefly luciferase gene in the pGL3 basic vector (Promega). The IRF3 and IRF3(5D) expression plasmids, pIRES-hrGFP/IRF3-Flag and pIRES-hrGFP/IRF3(5D)-Flag, were kindly provided by Professor Y. L. Lin (National Defense Medical Center, Taiwan, PR China).

Transfection and reporter gene assays. 293T cells were transfected using a calcium phosphate method (Mammalian Transfection kit; Promega) according to the manufacturer's instructions. Approximately 5×10^5 cells per well were co-transfected with 0.5 μg p125Luc, 0.1 μg of the constitutive *Renilla* luciferase construct pRL-TK (Promega), which served as an internal control, and 2.5 μg relevant expression plasmid. Where indicated, expression plasmids for IRF3(5D) (50 ng) and IRF3(50 ng) were included in the transfection mix. Cells were harvested at 24 h p.t. and lysed. Luciferase activity was determined using a dual-luciferase assay system (Promega) in a Turner Designs TD-20/20 luminometer.

Indirect immunofluorescence assay and confocal microscopy. HeLa cells were seeded onto glass coverslips in a 24-well plate and transfected with 0.8 μg HA-tagged ORF3b expression plasmids per well using Fugene HD regent (Roche). At 24 h p.t., cells were treated with 100 SeV HA units per well and fixed for 10 min at room temperature with 4 % paraformaldehyde at 8 h p.i. After three washes with PBS/0.1 % Tween 20, the cells were incubated with blocking buffer (PBS/3 % BSA) for 30 min and then with primary antibody, mouse mAb against the HA tag (Beyotime) and rabbit anti-IRF3 polyclonal antibody (Proteintech Group), for 1 h at 37 °C. Cells were washed three times and then incubated with FITC-conjugated goat anti-rabbit and TRITC-conjugated goat anti-mouse (Pierce) antibodies at a dilution of 1 : 100 for 30 min at 37 °C. After a further three washes, the slides were mounted with 50 % glycerol and observed under a Leica confocal microscope. For analysis of the localization of ORF3b, the immunofluorescence assay was carried out following the same procedure using mouse mAb against the HA tag and FITC-conjugated goat anti-mouse antibody (Pierce). Cells were then nuclear stained with Hoechst 33258 (Beyotime) for 5 min at room temperature. After washing, the cells were mounted with 50 % glycerol and observed under a Leica confocal microscope.

ACKNOWLEDGEMENTS

This work was funded by the State Key Program for Basic Research Grant (2011CB504700). We thank Dr Georg Kochs (Department of Virology, University of Freiburg, Germany) for providing influenza NS1 expression plasmid, Dr Yi-Ling Lin (Graduate Institute of Life Sciences, National Defense Medical Center, Taipei, Taiwan) for the IRF3 and IRF3(5D) expression plasmids and Mrs Jiaxin Liu (Wuhan Institute of Virology, Chinese Academy of Sciences) for technical support in confocal microscopy analysis.

REFERENCES

Basler, C. F., Mikulasova, A., Martinez-Sobrido, L., Paragas, J., Mühlberger, E., Bray, M., Klenk, H. D., Palese, P. & García-Sastre, A. (2003). The Ebola virus VP35 protein inhibits activation of interferon regulatory factor 3. *J Virol* **77**, 7945–7956.

Becker, M. M., Graham, R. L., Donaldson, E. F., Rockx, B., Sims, A. C., Sheahan, T., Pickles, R. J., Corti, D., Johnston, R. E. & other authors (2008). Synthetic recombinant bat SARS-like coronavirus is infectious in cultured cells and in mice. *Proc Natl Acad Sci U S A* **105**, 19944–19949.

Chan, W. S., Wu, C., Chow, S. C. S., Cheung, T., To, K.-F., Leung, W.-K., Chan, P. K. S., Lee, K.-C., Ng, H.-K. & other authors (2005). Coronaviral hypothetical and structural proteins were found in the intestinal surface enterocytes and pneumocytes of severe acute respiratory syndrome (SARS). *Mod Pathol* **18**, 1432–1439.

Chang, T. H., Liao, C. L. & Lin, Y. L. (2006). Flavivirus induces interferon-β gene expression through a pathway involving RIG-I-dependent IRF-3 and PI3K-dependent NF-κB activation. *Microbes Infect* **8**, 157–171.

Crameri, G., Todd, S., Grimley, S., McEachern, J. A., Marsh, G. A., Smith, C., Tachedjian, M., De Jong, C., Virtue, E. R. & other authors (2009). Establishment, immortalisation and characterisation of pteropid bat cell lines. *PLoS ONE* **4**, e8266.

Devaraj, S. G., Wang, N., Chen, Z., Chen, Z., Tseng, M., Barretto, N., Lin, R., Peters, C. J., Tseng, C. T. & other authors (2007). Regulation of IRF-3-dependent innate immunity by the papain-like protease domain of the severe acute respiratory syndrome coronavirus. *J Biol Chem* **282**, 32208–32221.

Fitzgerald, K. A., McWhirter, S. M., Faia, K. L., Rowe, D. C., Latz, E., Golenbock, D. T., Coyle, A. J., Liao, S. M. & Maniatis, T. (2003). IKKε and TBK1 are essential components of the IRF3 signaling pathway. *Nat Immunol* **4**, 491–496.

Freundt, E. C., Yu, L., Park, E., Lenardo, M. J. & Xu, X. N. (2009). Molecular determinants for subcellular localization of the severe acute respiratory syndrome coronavirus open reading frame 3b protein. *J Virol* **83**, 6631–6640.

Frieman, M., Ratia, K., Johnston, R. E., Mesecar, A. D. & Baric, R. S. (2009). Severe acute respiratory syndrome coronavirus papain-like protease ubiquitin-like domain and catalytic domain regulate antagonism of IRF3 and NF-κB signaling. *J Virol* **83**, 6689–6705.

García-Sastre, A. & Biron, C. A. (2006). Type 1 interferons and the virus–host relationship: a lesson in détente. *Science* **312**, 879–882.

Hiscott, J., Pitha, P., Genin, P., Nguyen, H., Heylbroeck, C., Mamane, Y., Algarte, M. & Lin, R. (1999). Triggering the interferon response: the role of IRF-3 transcription factor. *J Interferon Cytokine Res* **19**, 1–13.

Kamitani, W., Narayanan, K., Huang, C., Lokugamage, K., Ikegami, T., Ito, N., Kubo, H. & Makino, S. (2006). Severe acute respiratory syndrome coronavirus NSP1 protein suppresses host gene expression by promoting host mRNA degradation. *Proc Natl Acad Sci U S A* **103**, 12885–12890.

Kochs, G., García-Sastre, A. & Martínez-Sobrido, L. (2007). Multiple anti-interferon actions of the influenza A virus NS1 protein. *J Virol* **81**, 7011–7021.

Kopecky-Bromberg, S. A., Martínez-Sobrido, L., Frieman, M., Baric, R. A. & Palese, P. (2007). Severe acute respiratory syndrome coronavirus open reading frame (ORF) 3b, ORF 6, and nucleocapsid proteins function as interferon antagonists. *J Virol* **81**, 548–557.

Lau, S. K., Woo, P. C., Li, K. S., Huang, Y., Tsoi, H.-W., Wong, B. H., Wong, S. S., Leung, S.-Y., Chan, K.-H. & Yuen, K.-Y. (2005). Severe acute respiratory syndrome coronavirus-like virus in Chinese horseshoe bats. *Proc Natl Acad Sci U S A* **102**, 14040–14045.

Li, W., Shi, Z., Yu, M., Ren, W., Smith, C., Epstein, J. H., Wang, H., Crameri, G., Hu, Z. & other authors (2005). Bats are natural reservoirs of SARS-like coronaviruses. *Science* **310**, 676–679.

Liu, D. X. & Inglis, S. C. (1992). Internal entry of ribosomes on a tricistronic mRNA encoded by infectious bronchitis virus. *J Virol* **66**, 6143–6154.

Liu, D. X., Cavanagh, D., Green, P. & Inglis, S. C. (1991). A polycistronic mRNA specified by the coronavirus infectious bronchitis virus. *Virology* **184**, 531–544.

Randall, R. E. & Goodbourn, S. (2008). Interferons and viruses: an interplay between induction, signalling, antiviral responses and virus countermeasures. *J Gen Virol* **89**, 1–47.

Ren, W., Li, W., Yu, M., Hao, P., Zhang, Y., Zhou, P., Zhang, S., Zhao, G., Zhong, Y. & other authors (2006). Full-length genome sequences of two SARS-like coronaviruses in horseshoe bats and genetic variation analysis. *J Gen Virol* **87**, 3355–3359.

Shaw, M. L., García-Sastre, A., Palese, P. & Basler, C. F. (2004). Nipah virus V and W proteins have a common STAT1-binding domain yet inhibit STAT1 activation from the cytoplasmic and nuclear compartments, respectively. *J Virol* **78**, 5633–5641.

Tohya, Y., Narayanan, K., Kamitani, W., Huang, C., Lokugamage, K. & Makino, S. (2009). Suppression of host gene expression by NSP1 proteins of group 2 bat coronaviruses. *J Virol* **83**, 5282–5288.

Yuan, X., Yao, Z., Shan, Y., Chen, B., Yang, Z., Wu, J., Zhao, Z., Chen, J. & Cong, Y. (2005). Nucleolar localization of non-structural protein 3b, a protein specifically encoded by the severe acute respiratory syndrome coronavirus. *Virus Res* **114**, 70–79.